Ordering of C_{60} on Anisotropic Surfaces

D. Klyachko and D. M. Chen*
The Rowland Institute for Science, Cambridge, Massachusetts 02142
(Received 24 July 1995)

Based on our experimental observation of the uniaxial incommensurate C_{60} superlattices formed on Ge(100) and Si(100) surfaces, we show that the balance between the attractive and repulsive intermolecular forces plays the leading role in the ordering of a van der Waals overlayer on anisotropic substrates. A phenomenological expression for the superlattice parameters is derived and shown to be in good agreement with the experiments.

PACS numbers: 61.46.+w, 61.16.Ch, 64.70.Rh, 68.35.Bs

The interaction potential in a molecular solid [1], such as a noble gas solid or a C_{60} solid [2], is composed of a weak long-range attractive part and a strong short-range repulsive part. Together, these two parts play the crucial role in stabilizing the equilibrium lattice structure, since the attraction between distant neighbors associated with the long-range van der Waals forces must be counterbalanced by the nearest neighbor repulsion. In two-dimensional (2D) molecular adsorbates, however, the ordering is often governed by the competition between adsorbate-substrate and adsorbate-adsorbate interactions, and the intermolecular forces can be either predominantly attractive when the overlayer is under tension or repulsive when under compression [3]. As a result, incommensurate structures, both two-dimensional and uniaxial, are formed in numerous adsorption systems, including the well-studied noble gas adsorbates [4,5]. In this Letter, we report an experimental observation that shows that for large molecules such as C_{60} on a highly anisotropic surface the counterbalance of the intermolecular forces will play the leading role in determining the structural order of the adsorbate in one axis while the substrate-adsorbate interaction controls the other axis. This interaction scheme also leads to the formation of uniaxial incommensurate superlattices that exhibit varying degrees of long-range order.

Our observations were made on C_{60} overlayers on Ge(100)-(2 × 1) and Si(100)-(2 × 1) surfaces, using scanning tunneling microscopy (STM) and low energy electron diffraction (LEED). The experiments were conducted in a UHV system with a base pressure of 5×10^{-11} T. Clean Ge(100) and Si(100) surfaces were prepared by ion sputtering and thermal annealing at 760 and 1050 °C, respectively. All the surfaces contained no impurities within the detection limits of Auger electron spectroscopy, and showed sharp 2 × 1 superstructures in the LEED pattern. STM images of the clean surfaces revealed typical 2 × 1 dimer rows, which rotated 90° at each atomic step [6,7]. The average width of the terraces is ~500 Å. Immediately following the substrate preparation, C_{60} molecules were deposited at a rate of ~0.2 monolayer (ML) per minute from a Knudsen cell held at 480–510 °C. The commercial C_{60} powder from Mer Corp. contains 0.5% C_{70}. The substrate temperature was set to ~100 °C for Ge(100) and 150 °C for Si(100) in the beginning of the deposition, and gradually decreased to 40–50 °C at the end. The variation of the substrate temperature was intentionally chosen to reduce the nucleation rate during the initial stage of growth.

The above experimental procedures produce well-ordered C_{60} overlayer structures on the Ge(100) surface. Figure 1(a) is an STM image showing a C_{60} overlayer on two adjacent Ge terraces. The relative 90° rotation of the C_{60} lattices across the step is in close correspondence with the substrate dimer row rotation, indicating that the original surface structure remains intact beneath the C_{60} overlayer. STM images taken at submonolayer C_{60} coverage such as Fig. 1(b) show that all the C_{60} molecules reside in the troughs between the dimer rows. The LEED spots associated with the C_{60} structure begin to emerge when C_{60} coverage reaches $\frac{1}{3}$ ML. Figure 1(c) shows a well-developed LEED pattern for 1 ML C_{60} on the Ge(100) surface, where the typical one-half- and first-order Ge spots are marked. The eight spots on the innermost ring, forming the corners of two 90°-rotated rectangles, are the first-order spots of the two rota-

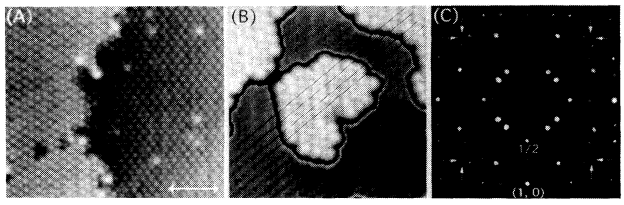

FIG. 1. (a) A 270 Å × 270 Å STM image taken with a tip bias of −3 V. It shows a C_{60} overlayer on two adjacent terraces of a Ge(100)-(2 × 1) surface with sparse brighter C_{70} impurities. The C_{60} lattice orientation rotates 90° across the atomic step. The arrows point to the dimer-row direction of the lower terrace. (b) A 160 Å × 175 Å STM image taken with a tip bias of +2.8 V. It shows that the C_{60} molecules in the domains are aligned with the troughs between the dimer rows of the uncovered surface. (c) 48 eV LEED pattern of two 90°-rotated domains of C_{60} rhombic lattices on the Ge(100)-(2 × 1) surface. The typical one-half-order and the first-order spots of the substrate are marked.

tional C_{60} domains. The remaining spots are either the second-order C_{60} spots, or are produced by the multiple scattering: once from the Ge substrate lattice, and once or twice from the C_{60} lattices.

By contrast, the STM image of Fig. 2(a) shows that the C_{60} molecules form only a partially ordered overlayer on the Si(100)-(2 × 1) surface. Nonetheless, the sizes of ordered C_{60} regions are sufficient to produce LEED patterns. Figure 2(b) displays two sets of the first-order C_{60} spots with 90° relative rotation. Together with the patterns obtained at other incident energies, we conclude that, except for the degraded quality, the LEED patterns for C_{60} on Si(100) are qualitatively the same as those for C_{60} on Ge(100). Locally, the C_{60} molecules form similar rhombic structure on both surfaces.

Apart from the 4% difference in lattice constants, the Si(100) and Ge(100) surfaces have otherwise identical anisotropic dimer-row structure. At first glance, the above results seem to be consistent with the model illustrated in Fig. 3, where the C_{60} molecules form an ideal 3 × 4 superstructure on top of the dimerized surface. This model was first assigned by Hashizume *et al.* to be the locally ordered C_{60} structure on the Si(100) surface [8]. However, careful measurements of the C_{60} lattice constants from the STM images and the LEED patterns reveal that while the C_{60} lattice is *commensurate* with the substrate in the direction normal to the troughs, it is *incommensurate* parallel to the troughs. In fact, the uniaxial incommensurability can be recognized in the LEED patterns. In Fig. 3(c), for example, the imaginary lines marked by the opposite arrow heads intersect the position of the two-thirds-order spots of the substrate lattice. For an ideal 3 × 4 overlayer structure, the seven spots immediately next to each of the lines should all fall

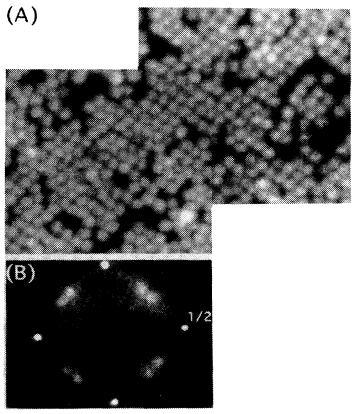

FIG. 2. (a) An STM image of a partially ordered C_{60} overlayer on the Si(100)-(2 × 1) surface. The combined dimension of the images is 250 Å × 200 Å, which was taken with a tip bias of −3.5 V. (b) 10 eV LEED pattern showing the one-half-order spots of the Si(100)-(2 × 1) surface and the first-order spots of the two-domain C_{60} overlayer.

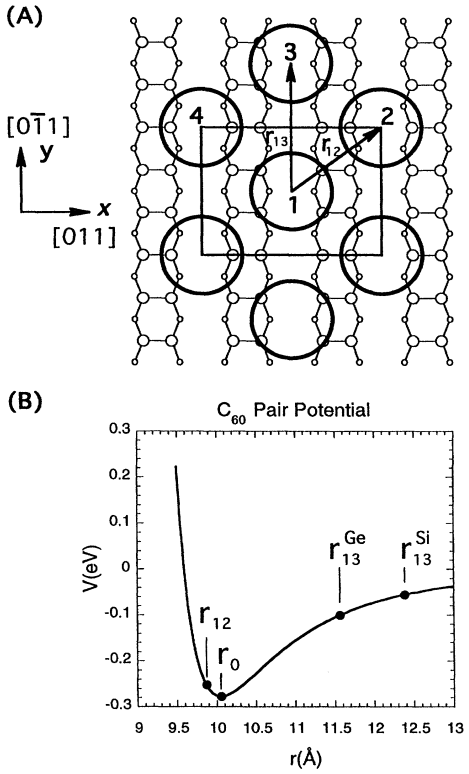

FIG. 3. (a) The ideal 3 × 4 C_{60} superlattice, marked by the rectangle, on the 2 × 1 dimer-row surface of Ge(100) or Si(100). The C_{60} molecules are represented by 7 Å large bold circles scaled in proportion to the substrate lattice. (b) The Girifalco potential for an isolated pair of C_{60} molecules separated at a distance of r. The positions for r_{12} and r_{13} in Table I are indicated.

on the lines. Compared with the respective 3 × 4 model, the intermolecular spacing r_{13} is ~3.5% smaller on Ge(100), but 8% larger on Si(100). Table I summarizes the basic C_{60} lattice parameters of the observed structures as well as the ideal 3 × 4 model. It is interesting to note that on Ge(100) surface the C_{60} lattice *contracts* along the troughs with respect to the ideal 3 × 4 structure while it *expands* on the Si(100) surface.

The above experimental observations raise two important questions. First, what drives these two systems to adopt uniaxially incommensurate rather than commensurate structures? And second, what causes these two rather similar adsorption systems to exhibit different degrees of long-range order?

In equilibrium, the potential energy of the C_{60} overlayer is at minimum, so that

$$\sum_i \frac{\partial}{\partial \mathbf{r}_i} V_{\mathrm{ms}}(\mathbf{r}_i) + \frac{1}{2} \sum_{i,j} \frac{\partial}{\partial \mathbf{r}_i} V_{\mathrm{mm}}(|\mathbf{r}_i - \mathbf{r}_j|) = 0, \quad (1)$$

where $\mathbf{r}_i$ is the position vector of the ith molecule, V_{ms} is the molecule-substrate interaction term, and V_{mm} is the intermolecular coupling term.

TABLE I. The C_{60} lattice parameters on Ge(100) and Si(100) surfaces from the measurements and the ideal 3×4 model shown in Fig. 3(a). δ is the % difference of r_{12} between the experimental value and that of the respective 3×4 model. The data in the last column are obtained from calculations as discussed in the text.

	Ge(100)-(3 × 4)	C_{60}/Ge Expt.	Si(100)-(3 × 4)	C_{60}/Si Expt.	C_{60}/Si Calc.
r_{24} (Å)	16.00	16.00	15.36	15.36	15.36
r_{12} (Å)	10.00	9.87	9.60	9.88	9.87
r_{13} (Å)	12.00	11.58	11.52	12.44 ± 1.5	12.40
δ	...	−3.5%	...	8.0%	7.6%

The fact that the molecules reside exclusively in the troughs suggests that the V_{ms} includes a relatively steep periodic potential along the x direction with the barriers on the dimer rows and the wells at the troughs. Normal to the troughs, $\partial V_{ms}(\mathbf{r}_i)/\partial x_i$ overrides intermolecular forces $\sum_j \partial V_{mm}(|\mathbf{r}_i - \mathbf{r}_j|)/\partial x_i$, and confines the molecule to the trough. Thus the molecular ordering in the x direction is defined by the x periodicity of V_{ms}.

This conclusion is supported by the detailed examination of the C_{60} registries at low coverage on both Ge(100) [9] and Si(100) [8,10] substrates. Almost all the isolated molecules are found to be adsorbed in the troughs and at the center of four adjacent dimers as molecule 1 in Fig. 3(a). At higher coverage, molecules adjust their position only along the trough. This further indicates that the V_{ms} has a weak dependence on y, compared with the intermolecular couplings, and

$$\partial V_{ms}(\mathbf{r}_i)/\partial y_i \ll \frac{1}{2} \sum_j \frac{\partial}{\partial y_i} V_{mm}(|\mathbf{r}_i - \mathbf{r}_j|) = 0 .$$

Under this assumption, all the molecules are equivalent, and Eq. (1) can be simplified to $\sum_j \partial V_{mm}(|\mathbf{r}_i - \mathbf{r}_j|)/\partial y_i = 0$; i.e., the y projections of the attractive and repulsive intermolecular forces exerted on each molecule are balanced. Considering only nearest and next nearest C_{60} pairs as shown in Fig. 3(a), we thus yield

$$2\frac{\partial V_{mm}(r_{12})}{\partial r_{12}} \frac{dr_{12}}{dr_{13}} + \frac{\partial V_{mm}(r_{13})}{\partial r_{13}} = 0 , \qquad (2)$$

where

$$r_{12} = \frac{1}{2}\sqrt{r_{13}^2 + r_{24}^2} \qquad (3)$$

and $V_{mm}(r)$ is the interaction potential of a pair of C_{60} molecules separated by r. Given the precise form of the C_{60} pair potential $V(r)$, Eqs. (2) and (3) determine the molecular ordering in the y direction.

The interaction potential for an isolated pair of C_{60} can be derived, to a good approximation, from the pairwise summation of the Lennard-Jones potential for all the carbon pairs [11–13]. Figure 3(b) shows the result obtained by Girifalco [12]. The Girifalco potential rises as $1/r^{10}$ at small distances, decays as $1/r^4$ at large distances, and gives an equilibrium distance r_0 of 10.06 Å. In a C_{60} solid, the attraction among higher order neighbors reduces r_0 to 10.02 Å [14]. When a pair of C_{60} is physisorbed on an uncorrugated surface, the shape of the pair potential has been shown to have no significant variation [13]. For systems where charge transfer between the molecules and the substrates takes place, the additional Coulomb repulsion would shift r_0 towards a higher value. For C_{60} on the Ge and Si surfaces, experimental findings available so far do not suggest an appreciable amount of charge transfer [8,15]. Thus we expect the essential features of the Girifaco potential mentioned above remain valid for the C_{60}-C_{60} coupling on Si(100) and Ge(100) surfaces.

These observations lead us to a satisfactory explanation for the present experimental results. As shown in Table I, the nearest C_{60}-C_{60} distance r_{12} in the ideal 3×4 structure on the Ge(100) is 10.0 Å, which, according to the Girifalco potential, suggests that molecules 1 and 2 would be close to their equilibrium positions. However, r_{13} is 12.0 Å, and hence the attraction between the 1-3 pair causes the molecules to move towards each other along the troughs. The contraction results in a reduced r_{12}, and 1-2 pairs experience an increasing repulsive force. When r_{12} is compressed to 9.87 Å ($r_{13} = 11.58$ Å), the attractive force is neutralized by the repulsive force, and the system reaches equilibrium. Therefore the ideal 3×4 C_{60} structure on the Ge(100) is unstable against contraction. On the other hand, for the ideal 3×4 structure on Si(100) surface, r_{12} is only 9.60 Å but r_{13} is 11.52 Å. This means there would be a net repulsive force inherent in this configuration. Consequently, the C_{60} molecules move away from each other along the troughs until the weakened repulsive force between the 1-2 pairs is counterbalanced by the attractive force exerted on the 1-3 pair. Thus the ideal 3×4 C_{60} structure on Si(100) is unstable against expansion. In both cases, the molecules are confined in the troughs by V_{ms} so that they are unable to adopt the closed hexagonal packing. Instead, they form rhombic lattices that are incommensurate along the troughs. It is noteworthy that both systems end up with the same compressed r_{12}, which is ~0.16 Å smaller than r_0 in a C_{60} solid [14].

A more quantitative treatment would require an accurate potential for the C_{60} on corrugated atomic surface, which is not yet available. Nevertheless, based on the character of strong short-range repulsion and weak long-range attraction of the C_{60} pair potential, the relationship

between the C_{60} lattice parameters r_{12} and r_{13} can be derived for these one-dimensionally-constrained systems. Consider a small change Δr_{24} of the dimer-row spacing introduced into the system described by the potential energy V. Both r_{12} and r_{13} will readjust so that the perturbed potential V' reaches a new minimum. Such an operation does not change the conditions that lead to Eq. (2). Thus taking the derivative of Eq. (2) with respect to r_{24} gives

$$\frac{dr_{13}}{dr_{24}} = -\frac{\partial^2[2V_{\rm mm}(r_{12}) + V_{\rm mm}(r_{13})]}{\partial r_{13}\partial r_{24}} \Big/ \frac{\partial^2[2V_{\rm mm}(r_{12}) + V_{\rm mm}(r_{13})]}{\partial r_{13}^2}. \quad (4)$$

Since the second derivatives of the pair potential is much larger in the repulsive regime than in the attractive regime, the right hand side of Eq. (4) equals approximately to $-r_{24}/r_{13}$ [16]. We then obtain a very simple result:

$$r_{12} = \text{const}. \quad (5)$$

Equation (5) implies that there is a universal compression limit in these systems, which is indeed observed. Using the experimental parameters for the C_{60} overlayer on Ge(100), Eqs. (3) and (5) allow us to predict the C_{60} overlayer lattice parameters on Si(100), and vice versa. As shown in the last column of Table I, the predictions are in good agreement with our measurements. Note that the above results do not depend on the detailed substrate structures and can, therefore, be applied to other van der Waals overlayers that are constrained similarly by an anisotropic substrate potential.

The preceding discussion concerns mainly the elementary structure of the superlattice. To address the different degrees of long-range order in the overlayers, we first note that the attractive potential V_{13} decreases from 100 meV on Ge(100) to 55 meV on the Si(100) surface, as marked in Fig. 3(b). This puts the attractive pair on Si(100) farther out in the less dispersive region of the potential and reduces the overall structural stability against thermal excitations and other factors. Along the troughs, $V_{\rm ms}$ varies gently with a periodicity of the dimer-dimer spacing. The incommensurability of the overlayer results in a phase shift of $\varphi/2\pi = 3n\delta$ from the local minimum for the nth molecule. In case of C_{60} on Si(100), the first nearest neighbor has $\varphi = 0.48\pi$, so that the substrate restoring force is in alliance with the rather weak van der Waals attractive force. For $n = \pm 2$, φ approaches π. Thus at $n = \pm 3$ a dislocation is likely to occur, and a typical ordered domain of C_{60} on the Si(100) should therefore have five molecules along the troughs. In comparison, the equivalent phase shift for C_{60} on Ge(100) is a factor of 2 less, and hence the C_{60} domain includes at least 10 molecules along the troughs.

In conclusion, we have observed uniaxial incommensurate C_{60} superlattices on Ge(100)-(2 × 1) and Si(100)-(2 × 1) surfaces. The formation of these structures is shown to result from the balance between C_{60} nearest neighbor repulsion and next nearest neighbor attraction in a highly anisotropic substrate potential. Quite remarkably, the expression for the superlattice parameters for these systems can be obtained phenomenologically without a detailed knowledge of the intermolecular interaction potential. We emphasize that the analytical approach presented here can be adapted to other van der Waals overlayers on anisotropic surfaces.

We thank M. Burns, J. Dunphy, and S. McDonald for valuable suggestions. This work is supported by the Rowland Institute for Science.

*To whom correspondence should be addressed.

[1] A. I. Kitaigorodsky, *Molecular Crystals and Molecules* (Academic, New York, 1973).
[2] S. Saito and A. Oshiyama, Phys. Rev. Lett. **66**, 2637 (1991).
[3] See various articles in *Ordering in Two Dimensions*, edited by Sunil K. Sinha (North-Holland, New York, 1980).
[4] R. J. Birgeneau and P. M. Horn, Science **232**, 329 (1986).
[5] P. Bak, V. L. Pokrovsky, and A. L. Talapov, in *Solitons*, edited by S. E. Trullinger, V. E. Zakharov, and V. L. Pokrovsky (North-Holland, Amsterdam, 1986).
[6] R. J. Hamers, R. M. Tromp, and J. E. Demuth, Phys. Rev. B **34**, 5343 (1986).
[7] J. A. Kubby, J. E. Griffith, R. S. Becker, and J. S. Vickers, Phys. Rev. B **36**, 6079 (1987).
[8] X.-D. Wang, T. Hashizume, H. Shinohara, Y. Saito, Y. Nishina, and T. Sakurai, Phys. Rev. B **47**, 15 923 (1993).
[9] D. Klyachko and Dongmin Chen, in Proceedings of the 8th International Conference on Scanning Tunneling Microscopy, 1995 (to be published).
[10] Dong Chen and Dror Sarid, Surf. Sci. **329**, 206 (1995).
[11] Y. Guo, N. Karasawa, and W. A. Goddard, Nature (London) **351**, 464 (1991).
[12] L. A. Girifalco, J. Phys. Chem. **96**, 858 (1992).
[13] CH. Girard, Ph. Lambin, A. Dereux, and A. A. Lucas, Phys. Rev. B **49**, 11 425 (1994).
[14] P. A. Heiney, J. E. Fisher, A. R. McGhie, W. J. Romanow, A. M. Denenstein, J. P. McCauley, and A. B. Smith, Phys. Rev. Lett. **66**, 2911 (1991).
[15] Hang Xu, thesis, Harvard University, 1994.
[16] For the present two systems, $V_{\rm mm}(r_{13})$ is always attractive and $V_{\rm mm}(r_{12})$ is always repulsive. Thus the second derivatives of the latter are the dominating terms. Furthermore, the changes of partial derivative $\partial/\partial r_{13}$ and $\partial/\partial r_{24}$ to $\partial/\partial r_{12}$ introduce additional terms involving the first derivative of $V_{\rm mm}(r_{12})$, which can be shown using Girifalco potential, for example, to be an order of magnitude less than the second derivative.

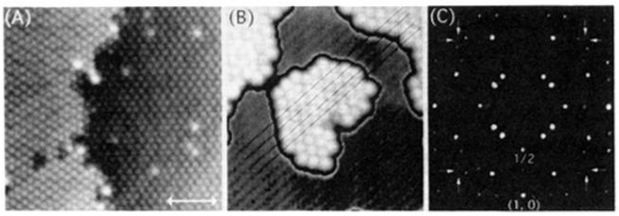

FIG. 1. (a) A 270 Å × 270 Å STM image taken with a tip bias of −3 V. It shows a C_{60} overlayer on two adjacent terraces of a Ge(100)-(2 × 1) surface with sparse brighter C_{70} impurities. The C_{60} lattice orientation rotates 90° across the atomic step. The arrows point to the dimer-row direction of the lower terrace. (b) A 160 Å × 175 Å STM image taken with a tip bias of +2.8 V. It shows that the C_{60} molecules in the domains are aligned with the troughs between the dimer rows of the uncovered surface. (c) 48 eV LEED pattern of two 90°-rotated domains of C_{60} rhombic lattices on the Ge(100)-(2 × 1) surface. The typical one-half-order and the first-order spots of the substrate are marked.

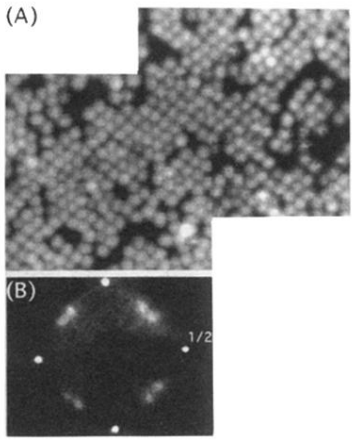

FIG. 2. (a) An STM image of a partially ordered C_{60} overlayer on the Si(100)-(2 × 1) surface. The combined dimension of the images is 250 Å × 200 Å, which was taken with a tip bias of −3.5 V. (b) 10 eV LEED pattern showing the one-half-order spots of the Si(100)-(2 × 1) surface and the first-order spots of the two-domain C_{60} overlayer.